CROSS FLOW OVER CYLINDERS WITH TWO STEPWISE DISCONTINUITIES IN DIAMETER

Christopher Morton
Department of Mechanical & Mechatronics Engineering
University of Waterloo
200 University Avenue West, Waterloo, Ontario, N2L 3G1, Canada
cmorton@uwaterloo.ca

Serhiy Yarusevych
Department of Mechanical & Mechatronics Engineering
University of Waterloo
200 University Avenue West, Waterloo, Ontario, N2L 3G1, Canada
syarus@uwaterloo.ca

ABSTRACT

Vortex shedding in the wake of dual step cylinders was investigated experimentally using flow visualization and Laser Doppler Velocimetry (LDV). The dual step cylinder model consists of a small diameter cylinder (d) and a large diameter cylinder (D) mounted at the mid-span of the small cylinder. Experiments were performed for Re_D = 1050, D/d = 2, and large cylinder aspect ratios in the range of $0.2 \leq L/D \leq 17$. Hydrogen bubble flow visualization results show that the wake development is highly dependent on the aspect ratio of the large cylinder, L/D. Spectral analysis of streamwise velocity signals obtained in the dual step cylinder wake was used to estimate the shedding frequency variation along the model span. The results identify four distinct flow regimes: (i) for $L/D \geq 17$, three vortex shedding cells form in the wake of the large cylinder, one central cell and two cells of lower frequency, (ii) for $7 < L/D \leq 14$, a single vortex shedding cell forms in the wake of the large cylinder, whose shedding frequency decreases with decreasing L/D, (iii) for $2 \leq L/D < 7$, large cylinder vortex shedding is highly three-dimensional, and the frequency of the shedding continues to decrease with L/D, (iv) for $0.2 \leq L/D \leq 1$, the large cylinder induces vortex dislocations between small cylinder vortices whose frequency of occurrence decreases with L/D.

INTRODUCTION

Fluid flow over cylindrical bodies is relevant to the design of civil structures and mechanical engineering systems, e.g., bridges, offshore structures, towers, wind turbines, and tube-and-shell heat exchangers. Of particular importance is the understanding of unsteady loading characteristics, vibrations, noise generation, and other phenomena, all of which are highly dependent on the flow development. Consequently, the flow development over various cylindrical geometries (e.g., uniform cylinders, cylinders with stepwise discontinuities in diameter, and free-end cylinders) has been the focus of a number of investigations over the past several decades (e.g., Williamson, 1989; Dunn and Tavoularis, 2006; Zdravkovich, 1989). For non-uniform cylindrical geometries, vortex shedding has been shown to occur in distinct cells of constant frequency. The current study is focused on the flow development over cylinders with two stepwise discontinuities in diameter along the span (Fig. 1). For this geometry, the wake development, which to the best of the authors' knowledge has not been investigated in detail, is expected to be similar to that observed for a single step cylinder and a cylinder with free ends.

The wake of a single step cylinder has been shown to contain three distinct spanwise vortex cells for D/d > 1.55 and $Re_D \gtrsim 100$ (Lewis and Gharib, 1992). Dunn and Tavoularis (2006) classify these cells as follows: (i) the S-cell, vortex shedding from the small cylinder; (ii) the L-cell, vortex shedding from the large cylinder; (iii) the N-cell, distinct vortex shedding in the region between the S-cell and L-cell. The N-cell has the lowest of the three shedding frequencies, with the ratio of the N-cell to L-cell frequencies (f_N/f_L) reported to range from 0.84 to 0.97 (Dunn and Tavoularis, 2006; Lewis and Gharib, 1992; Morton and Yarusevych, 2010). The N-cell exhibits a cyclic behavior, such that its

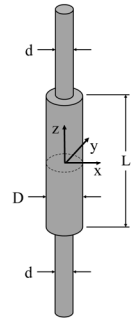

Figure 1. Dual step cylinder geometry.

spanwise extent fluctuates periodically which may be linked to downwash fluctuations occurring in the N-cell vortex formation region (Dunn and Tavoularis, 2006).

For a cylinder with two free ends, the experimental results of Zdravkovich et al. (1989) and numerical findings of Inoue and Sakuragi (2008) indicate a strong dependence of the wake topology on the aspect ratio (L/D). Inoue and Sakuragi (2008) investigated numerically the flow over a cylinder with two free ends for $40 \leq Re_D \leq 300$ and $0.5 \leq L/D \leq 100$. For $L/D \gtrsim 20$, they identify three wake vortex shedding cells: one cell located near the mid-span and two cells of lower frequency located near the cylinder ends.

Although the flow development past a dual step cylinder has not been investigated in detail, the results of experimental studies by Williamson (1992) and Nakamura and Igarashi (2008) provide insight into the dual step cylinder wake topology. Williamson (1992) investigated the development of vortex dislocations by attaching a ring (diameter D) to the mid-span of a uniform circular cylinder (diameter d), i.e., forming a dual step cylinder. Flow visualization images and wake velocity measurements were obtained for $Re_d \leq 200$, D/d = 1.1 and 1.5, and L/D = 0.5. The results show that, by controlling the shedding frequencies on both sides of the ring via end plate adjustments, two distinct patterns of periodic vortex dislocations can be induced (Williamson, 1992). In particular, when the vortex shedding frequencies match, vortex dislocations on each side of the ring occur at the same frequency and form in phase. In contrast, when the shedding frequencies differ, so do the frequencies of the dislocations on each side of the ring. In addition, the results presented in Williamson (1992) for D/d = 1.1, 1.5, and 2, imply that the frequency of vortex dislocations decreases with decreasing D/d.

Nakamura and Igarashi (2008) used multiple, evenly-spaced rings to reduce aerodynamic forces on a circular cylinder. Their study was completed for $3000 \leq Re_D \leq 38{,}000$ and a range of aspect ratios (L/D), diameter ratios (D/d), and ring spacings (P/D). For a range of geometric parameters (L/D, D/d, P/D), drag reduction was observed and was attributed to delayed flow separation on the attached rings.

The present study is motivated by the need for insight into vortex shedding occurring in the wake of a dual step cylinder. The objective is to examine the effect of the large cylinder aspect ratio (L/D) on vortex shedding characteristics.

EXPERIMENTAL SETUP

Experiments involving dual step cylinders were carried out in a water flume facility at the University of Waterloo. Dual step cylinders were mounted between circular endplates (Fig. 2) in order to reduce end effects (West and Fox, 1990). The geometric parameters of the investigated dual step cylinder models are shown in Table I. Wake vortex shedding was visualized using a hydrogen bubble technique. Hydrogen bubbles were produced on a thin (0.09 mm diameter) stainless steel wire mounted approximately 0.2D upstream of the cylinder along its entire span. Spanwise vortices on one side of the wake were illuminated with a laser sheet positioned in the x-z plane at $y/D \approx 0.4$. It was verified experimentally that buoyancy had a negligible effect on the motion of hydrogen bubbles within the near wake region of interest. Flow visualization images were obtained with a Nikon D300 camera. In addition, another camera was used to record videos simultaneously with sequences of still images at a frame rate of approximately 15 Hz (about five times the highest shedding frequency). Flow visualization videos were used to estimate the vortex shedding frequency and provide insight into overall wake development. For estimating the shedding frequency, video records capturing more than 250 vortex shedding cycles were analysed.

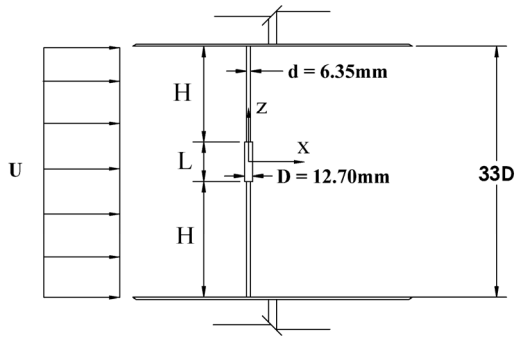

Figure 2. Experimental arrangement.

The streamwise velocity component (u) was measured using a Laser Doppler Velocimetry (LDV) system. Measurements were conducted five local diameters (d or D) downstream of the dual step cylinder. The water used for the experiments contains natural seeding particles allowing for mean data acquisition rates greater than 50 Hz. All wake velocity data acquired were re-sampled at a fixed frequency of 30 Hz using the sample-and-hold technique (Adrian and Yao, 1987). For spectral analysis, each re-sampled velocity signal was divided into 24 non-overlapping blocks, each containing 1024 data points. The discrete Fourier transform was used to compute velocity spectra, with a frequency resolution of approximately ±0.0012 fD/U. It was verified that the Strouhal number (St) estimates obtained based on flow visualization video records and those from spectral analysis of velocity data match to within the experimental uncertainty of about 1.5%.

RESULTS

Flow over a dual step cylinder was investigated for Re_D = 1050, D/d = 2, and $0.2 \leq L/D \leq 17$. The wake development was found to depend significantly on the large cylinder aspect ratio (L/D). Four distinct regimes identified in this study are discussed in this section. The L/D ranges defined for each regime are approximated based on the values of the large cylinder aspect ratios investigated (Table 1). Unless specified

Table 1. Investigated dual step cylinder parameters. Note, for all models, D/d = 2.

L/D	17	14	10	7	5	3	2	1	0.2
H/D	16	19	23	26	28	30	31	32	33

otherwise, the main vortex shedding cells in the wake of the large and small cylinders are referred to as the L-cell and the S-cell, respectively.

Regime I (L/D = 17)

The flow development over a dual step cylinder for L/D = 17 is illustrated in Fig. 3a. Flow visualization (Fig. 3a) shows that three vortex cells form in the wake of the large cylinder: the L-cell, located near the mid-span of the large cylinder, and two N-cells of lower shedding frequency positioned near each step. S-cells form in the small cylinder wake above and below the large cylinder. Figure 3b shows the variation of the dimensionless vortex shedding frequency across the cylinder span. At a given z/D location, each data point in Fig. 3b corresponds to the frequency of the dominant peak in the corresponding velocity spectrum. The results illustrate the variation of the shedding frequency across the span of the dual step cylinder. The S-cell is the principal frequency-centered activity over the entire span of the small cylinder, with a dimensionless frequency of fD/U = 0.390 for z/D ≥ 8, and fD/U = 0.379 for z/D ≤ −8. The N-cell frequency-centered activity is dominant in the two large cylinder wake regions downstream of the step discontinuities, with a dimensionless frequency of fD/U = 0.191 near the top step and fD/U = 0.189 near the bottom step (Fig. 3b). The L-cell frequency, fD/U = 0.195, is the principle frequency in the core of the large cylinder wake. The following time-average locations of cell boundaries are identified in Fig. 3b: (i) the N-S boundary, z/D ≈ ±7.5, and (ii) the N-L boundary, z/D ≈ ±3. These locations correspond to the measurement planes where a change in the dominant spectral frequency occurs. Within about one large cylinder diameter on either side of the identified cell boundaries, streamwise velocity spectra show two peaks centred at the dimensionless frequencies of the adjacent vortex cells. Dunn and Tavoularis (2006) report a similar trend for a single step cylinder of the same D/d. Streamwise velocity spectra at five locations along the dual step cylinder span are shown in Fig. 4. Figures 4a, 4c, and 4e depict streamwise velocity spectra within the S-cell, N-cell, and L-cell, respectively. Figures 4b and 4d show velocity spectra at the N-S boundary and N-L boundary, respectively, where the vortex shedding frequencies of the two adjacent vortex cells can be identified. It should be noted that the Strouhal numbers of the S-cell and the L-cell are slightly lower than those expected for a uniform circular cylinder at the corresponding Reynolds numbers (St=0.200 and St = 0.205, respectively). This is attributed to two factors: (i) oblique shedding occurs in the S-cell and L-cell, which is known to reduce the measured vortex shedding frequency (Williamson, 1989), and (ii) lower aspect ratio cylinders produce lower St (Norberg, 1994).

Analysis of flow visualization videos revealed that the locations of the cell boundaries fluctuate with time. This is illustrated in Fig. 5, which shows a sequence of flow visualization images for a dual step cylinder with L/D = 17. Similar to the case of a single step cylinder (Dunn and Tavoularis, 2006), the N-cells develop cyclically near each of the two steps. Figure 5a shows nearly parallel vortex shedding in the wake of the large cylinder. Over time, vortices in the

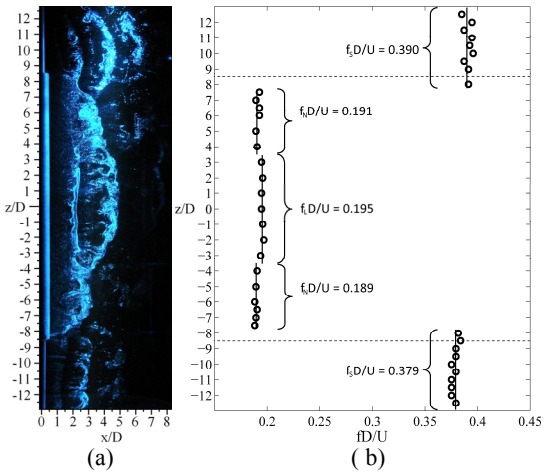

(a) (b)

Figure 3. Flow development in the wake of a dual step cylinder for L/D = 17: (a) hydrogen bubble flow visualization, and (b) dimensionless dominant wake frequency across the span.

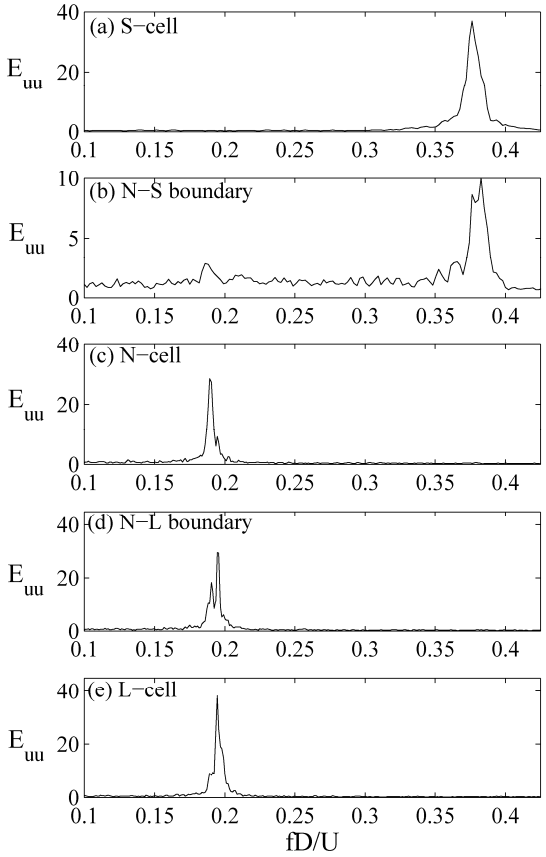

Figure 4. Velocity spectra at five locations along the span of a dual step cylinder with L/D = 17: (a) z/D = 12, (b) z/D = 8.0, (c) z/D = 5, (d) z/D = 3, and (e) z/D = 0.

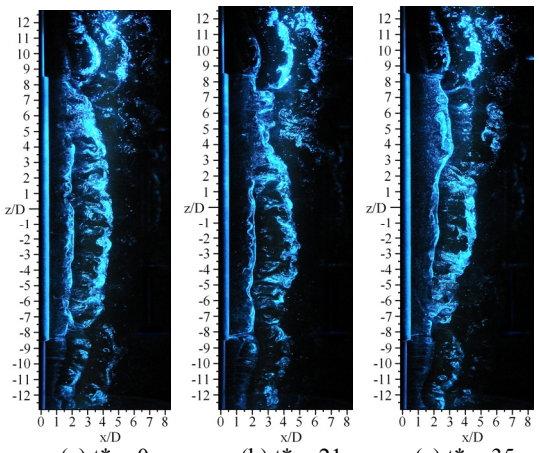

(a) t* = 0 (b) t* = 21 (c) t* = 35

Figure 5. N-cell development in the wake of a dual step cylinder for L/D = 17. Note, t* is the number of shedding periods of small cylinder vortices.

large cylinder wake move out of phase such that a distinct vortex shedding cell, an N-cell, can be identified within 3.0 ≤ z/D ≤ 8.0 in Fig. 5b. The N-cell vortices continue to move out of phase with the L-cell vortices until a vortex dislocation occurs (e.g., z/D = 2 and x/D = 3 in Fig. 5c). After a few L-cell shedding cycles, the N-cell vortices re-align with the large cylinder vortices, marking the beginning of the next N-cell cycle. Video records showed that the N-cell near the top step and the N-cell near the bottom step move in and out of phase due to the slight difference in their shedding frequency (Fig. 3b). The image sequence in Fig. 5 shows N-cell development near the bottom step, while Fig. 3a shows two N-cells forming in phase. Williamson (1992) observed a similar phenomenon for vortex dislocations induced by a ring attached to a uniform cylinder.

The results presented suggest that, in this flow regime, wake topology of a dual step cylinder within z/D > 0 and z/D < 0 is similar to that of a single step cylinder. For cylinders with two free ends, Inoue and Sakuragi (2008) report that a similar cellular vortex shedding pattern occurs for L/D > 20. This suggests that the flow regime observed in the dual step cylinder wake at L/D = 17 will likely persist for higher aspect ratios.

Regime II (7 < L/D ≤ 14)

In this flow regime, vortex shedding from the large cylinder occurs in a single cell (L-cell). As depicted in Fig. 6a, L-cell vortices are shed nearly parallel to the cylinder axis, and form vortex connections with S-cell vortices. Figure 6b shows the variation of dimensionless shedding frequency across the dual step cylinder span for L/D = 10. In agreement with the flow visualization image (Fig. 6a), a single dominant frequency exists in the wake of the large cylinder for about −4 ≤ z/D ≤ 4. A change in dominant frequency occurs at z/D ≈ ±4, defining the time-average locations of L-S boundaries.

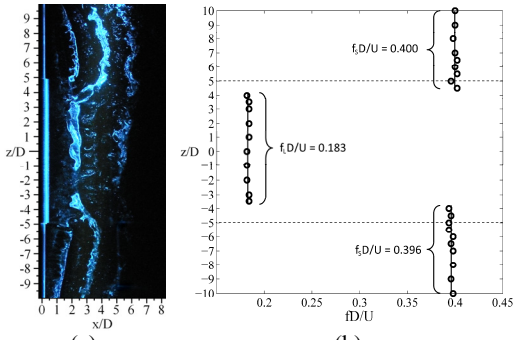

(a) (b)

Figure 6. Flow development in the wake of a dual step cylinder for L/D = 10: (a) hydrogen bubble flow visualization, and (b) dimensionless dominant wake frequency across the span.

The L-S boundaries are also visible on the large cylinder side of the step in the hydrogen bubble flow visualization (Fig. 6a). Similar to Regime I, within the S-cell and L-cell, a single dominant peak is observed in the streamwise velocity spectra (Figs. 7a and 7c). In contrast, near cell boundaries, streamwise velocity spectra show two peaks corresponding to the L-cell and S-cell shedding frequencies (Fig. 7b).

Analysis of flow visualization showed that the L-cell dimensionless frequency decreases with L/D from fD/U ≈ 0.193 (L/D = 14) to fD/U ≈ 0.175 (L/D = 7). Inoue and Sakuragi (2008) report a comparable shedding regime in the wake of a cylinder with two free ends for 10 ≤ L/D < 20, where the shedding frequency also decreases with aspect ratio. It should be noted that the Strouhal number of the S-cells in

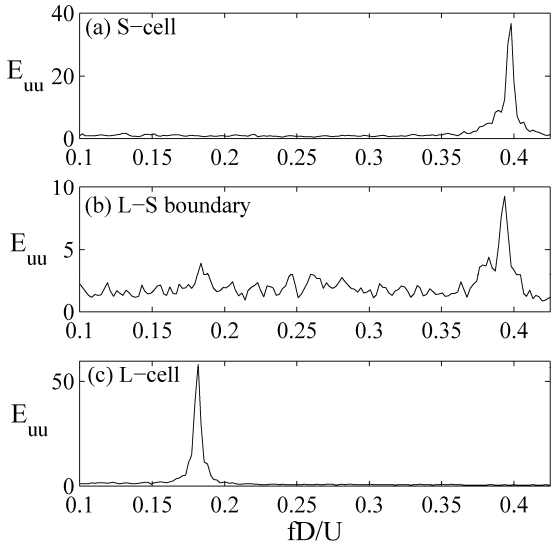

Figure 7. Velocity spectra at three locations along the span of a dual step cylinder for L/D = 10: (a) z/D = 10, (b) z/D = 4.5, (c) z/D = 0.

Regime II matches the dimensionless frequency expected for a uniform cylinder at the same Reynolds number (Norberg, 2003). The change in dimensionless frequency of the S-cells between Regime I and Regime II is attributed to the increase in the small cylinder aspect ratios (Norberg, 1994), as shown in Table 1.

Regime III (2 ≤ L/D < 7)

In this regime, vortex shedding in the wake of the large cylinder is difficult to identify via flow visualization (Fig. 8a). However, a detailed analysis of flow visualization video records revealed that vortices do form in the large cylinder wake but get distorted into hairpin-like structures. For laminar shedding from a cylinder with two free ends, similar three-dimensional hairpin shedding was observed by Inoue and Sakuragi (2008) for L/D < 10. Figure 8b shows the variation of the dimensionless frequency across the span of a dual step cylinder in Regime III. Despite being deformed, large cylinder wake vortices are characterized by a distinct dimensionless frequency, fD/U = 0.162. This is the dominant frequency within −2 ≤ z/D < 2, similar to the case of Regime II. In agreement with the trends reported for Regime II, the dimensionless frequency of the L-cell decreases with L/D in Regime III, with fD/U = 0.162 for L/D = 5 (Fig. 8b) and fD/U ≈ 0.135 for L/D = 2.

Comparing the results presented in Figs. 8a and 8b, it can be seen that there is variation in the location of the boundary between large cylinder and small cylinder wake. The flow visualization results indicate that the L-S cell boundary is located on the small cylinder side of the wake (Fig. 8a for x/D < 3) while wake velocity measurements conducted at x/D = 5 place the boundary on the large cylinder side of the wake (Fig. 8b). This suggests that, as the wake develops, small cylinder vortices are entrained into the large cylinder wake, so that the time-average position of the cell boundary changes with x/D.

Streamwise velocity spectra representative of those observed within each vortex cell and near the cell boundaries are shown in Fig. 9. Inside the vortex cells, well defined peaks centred at the S-cell and L-cell shedding frequencies can be seen in Figs. 9a and 9c, respectively. Near the cell boundary (Fig. 9b), the energy content of the spectral peaks at the S-cell and L-cell shedding frequencies is reduced significantly. In addition, another peak can be seen in the spectrum at fD/U ≈ 0.21, which approximately matches the dimensionless frequency expected for a uniform cylinder (of diameter D) at the investigated Re_D (Norberg, 2003). The physical phenomenon associated with velocity fluctuations at this dimensionless frequency needs to be investigated in the future.

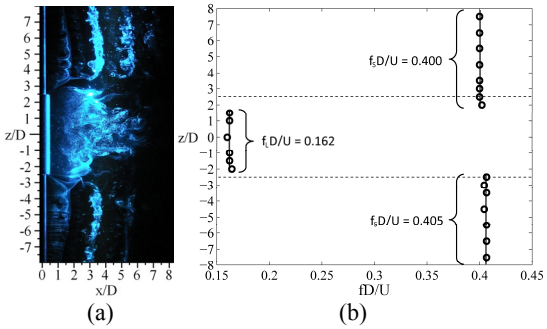

Figure 8. Flow development in the wake of a dual step cylinder for L/D = 5: (a) hydrogen bubble flow visualization, and (b) dimensionless dominant wake frequency across the span.

Regime IV (0.2 ≤ L/D ≤ 1)

When the aspect ratio of the large cylinder is reduced to L/D = 1, no distinct vortex shedding cell can be observed in the large cylinder wake. Flow visualization results (Fig. 10a) suggest that S-cell vortices span across the wake of the large cylinder. In this regime, the large cylinder induces vortex dislocations within the S-cells, similar to the results of Williamson (1992). This is illustrated in Fig. 10a, where S-cell vortices S3 and S3* form vortex connections across the wake of the large cylinder, while vortices S1 and S1* do not form such a connection. Vortex dislocations are manifested by two S-cell vortices forming half-loop connections within each of the two S-cells, e.g., vortices S1 and S2, and S1* and S2* in Fig. 10a. Analysis of video records showed that, for the two aspect ratios investigated in Regime IV (L/D = 0.2 and 1), the frequency of occurrence of vortex dislocations decreases with L/D.

Figure 11 depicts streamwise velocity spectra within the S-cell and in the wake of the large cylinder for L/D = 1. Peaks centered at the S-cell shedding frequency appear in all spectra presented. In addition, broad peaks centred at fD/U ≈ 0.203 are observed in the spectra pertaining to the wake of the large cylinder (Fig. 11b and 11c). Although the physical phenomenon responsible for the occurrence of these spectral peaks is yet to be explained, their dimensionless frequency is substantially higher than that associated with the L-cell in

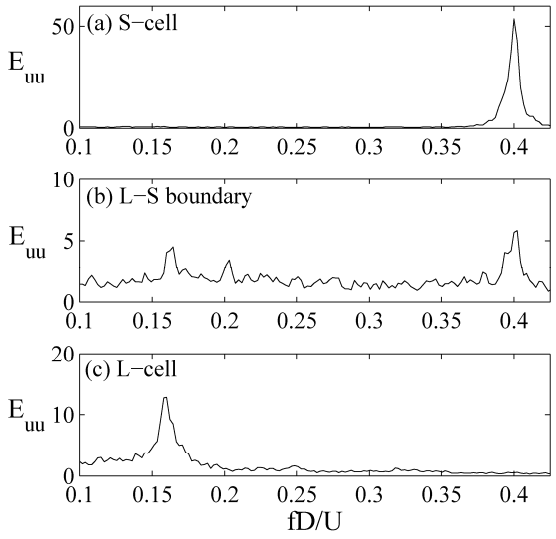

Figure 9. Velocity spectra at three locations along the span of a dual step cylinder for L/D = 5: (a) z/D = 7.5, (b) z/D = 2, and (c) z/D = 0.

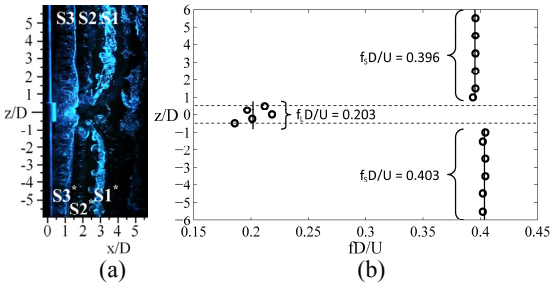

Figure 10. Flow development in the wake of a dual step cylinder for L/D = 1: (a) hydrogen bubble flow visualization, and (b) dimensionless dominant wake frequency across the span.

Regime III. In addition, the associated frequency-centred activity is less coherent, as evidenced by the broad peaks in Figs. 11b and 11c and the variation in the dominant frequency with z/D (Fig. 10b). At much lower Reynolds numbers (Re ~ 10^2), Williamson (1992) detected a similar frequency-centred activity in the wake of a ring attached to a uniform cylinder. His flow visualization results do not shed light on the underlying physical phenomenon. However, Williamson's measurements show that vortex dislocations occur at the frequency corresponding to the difference of the S-cell frequency and the ring frequency.

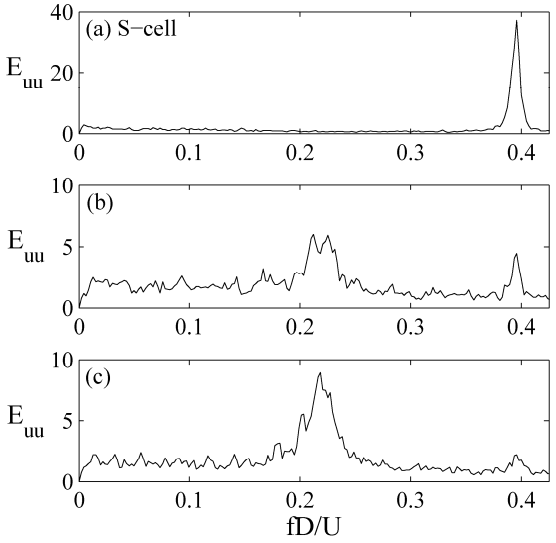

Figure 11. Velocity spectra at three locations along the span of a dual step cylinder for L/D = 1: (a) z/D = 5.5, (b) z/D = 0.5, and (c) z/D = 0.

CONCLUSIONS

Vortex shedding in the wake of a dual step cylinder was investigated experimentally for $Re_D \approx 1050$, D/d = 2, and $0.2 \leq L/D \leq 17$. Flow visualization and velocity measurements were utilized to characterize wake vortex shedding. The wake development was found to depend significantly on the large cylinder aspect ratio (L/D). For the cases investigated, four distinct vortex shedding regimes were identified.

For $L/D \geq 17$, the flow development within $z/D > 0$ or $z/D < 0$ is similar to that found for a single step cylinder (e.g., Dunn and Tavoularis, 2006). Specifically, in the wake of the large cylinder, a lower frequency vortex shedding cell (N-cell) forms near a stepwise discontinuity and another cell (L-cell) forms away from the step.

For $7 < L/D \leq 14$, vortex shedding from the large cylinder occurs in a single cell (L-cell). The shedding frequency of the L-cell decreases with L/D, agreeing with the trend reported for free end cylinders (Inoue and Sakuragi, 2008).

For $2 \leq L/D < 7$, vortices shed from the large cylinder deform substaintially, attaining a harpin-like shape in the near wake. These vortices are characterized by a distinct dimensionless L-cell frequency, which continues to decrease with L/D.

For $0.2 \leq L/D \leq 1$, the results show that the large cylinder induces dislocations between the vortices shed from the small cylinders. Analysis of flow visualization videos suggests that the dislocation frequency decreases with L/D.

REFERENCES

Dunn, W., Tavoularis, S., 2006, "Experimental studies of vortices shed from cylinders with a step-change in diameter", *Journal of Fluid Mechanics*, Vol. 555, pp.409-437.

Inoue, O., Sakuragi, A., 2008, "Vortex shedding from a circular cylinder of finite length at low Reynolds numbers", *Physics of Fluids*, Vol. 20, No. 033601.

Lewis, C.G., Gharib, M., 1992, "An exploration of the wake three dimensionalities caused by a local discontinuity in cylinder diameter", *Physics of Fluids A*, Vol. 4, pp. 104-117.

Morton, C., Yarusevych, S., 2010, "Vortex shedding in the wake of a step cylinder", *Physics of Fluids*, Vol. 22, No. 083602.

Nakamura, H., Igarashi, T., 2008, "Omnidirectional reductions in drag and fluctuating forces for a circular cylinder by attaching rings", *Journal of Wind Engineering and Industrial Aerodynamics*, Vol. 96, pp.887-899.

Norberg, C., 1994, "An experimental investigation of the flow around a circular cylinder: influence of aspect ratio", *Journal of Fluid Mechanics*, Vol. 258, pp. 287-316.

Norberg, C., 2003, "Fluctuating lift on a circular cylinder: review and new measurements", *Journal of Fluids and Structures*, Vol. 17, pp.57-96.

West, G.H., Fox, T.A., 1990 "On the use of end plates with circular cylinders", *Experiments in Fluids*, Vol. 9, pp.237-239.

Williamson, C.H.K., 1989, "Oblique and parallel modes of vortex shedding in the wake of a circular cylinder at low Reynolds numbers", *Journal of Fluid Mechanics*, Vol. 206, pp.579-627.

Williamson, C.H.K., 1992, "The natural and forced formation of spot-like 'vortex dislocations' in the transition of a wake" *Journal of Fluid Mechanics*, Vol. 243, pp.393-441.

Zdravkovich, M.M., Brand, V.P., Mathew, G., Weston, A., 1989, "Flow past short circular cylinders with two free ends", *Journal of Fluid Mechanics*, Vol. 203, pp.557-575.